Bulletin of Mathematical Biology (1999) **01**, 1–20

FAST SUBSYSTEM BIFURCATIONS IN STRONGLY COUPLED HETEROGENEOUS COLLECTIONS OF EXCITABLE CELLS

M. PERNAROWSKI
DEPARTMENT OF MATHEMATICAL SCIENCES
MONTANA STATE UNIVERSITY
BOZEMAN, MT 59717
EMAIL: PERNAROW@MATH.MONTANA.EDU †

A continuum model for a heterogeneous collection of excitable cells electrically coupled through gap junctions is introduced and analyzed using spatial averaging, asymptotic and numerical techniques. Heterogeneity is modelled by imposing a spatial dependence on parameters which define the single cell model and a diffusion term is used to model the gap junction coupling. For different parameter values single cell models can exhibit bursting, beating and a myriad of other complex oscillations. A procedure for finding asymptotic estimates of the thresholds between these (synchronous) behaviors in the cellular aggregates is described for the heterogeneous case where the coupling strength is strong. This procedure is tested on a model of a strongly coupled heterogeneous collection of bursting and beating cells. Since isolated pancreatic β-cells have been observed to both burst and beat, this test of the spatial averaging techniques provides a possible explanation to measured discrepancies between the electrical activities of isolated β-cells and coupled collections (islets) of β-cells.

Keywords: heterogeneity, bursting, beating, β-cells, fast subsystems

1. INTRODUCTION

In many instances, intercellular ionic currents pass through small porous protein structures called gap junctions. Gap junction coupling has been identified in the liver, smooth muscles, the epithelia, myocardial tissue, the pancreas and blastomeres (Hille, 1992). Some of the cells in these tissues are electrically excitable and in most cases the coupling due to gap junctions is passive. If two cells m and n with respective transmembrane potentials v_m and v_n are coupled by gap junctions this current is often modelled by

$$I_{m,n} = g_{m,n}(v_m - v_n) \quad , \tag{1}$$

†THIS WORK WAS SUPPORTED BY THE NATIONAL SCIENCE FOUNDATION GRANT DMS-97-04-966

0092-8240/99/010001 + 20 $17.00/0 mb99????

where $g_{m,n}$ is the net conductance of all such gap junctions connecting the two cells. If the individual transmembrane currents of each cell are known then an appropriate model for the m-th cell is:

$$C_m \frac{dv_m}{dt} = -\sum_X I_X(v_m, \vec{w}_m) - \sum_{n=1}^{N} g_{m,n}(v_m - v_n) \ , \tag{2}$$

$$\frac{d\vec{w}_m}{dt} = W_m(v_m, \vec{w}_m), \vec{w}_m \in \mathbb{R}^M. \tag{3}$$

The first of these equations represents a balance of capacitive currents (left side) and currents through ionic and gap junction channels (right side). The parameter C_m is the total capacitance of the cell, I_X are the transmembrane currents through ionic channels (e.g. voltage-gated sodium, calcium inactivated potassium), and $\vec{w}_m$ are variables which describe gating and other regulatory effects for each ionic channel of type X. Often, many of these variables evolve slowly. Lastly, cell to cell heterogeneity is modelled by imposing a subscript m dependence on the parameters defining I_X and W_m.

Models of the form (2)-(3) have been used to study propagation failure in myocardial tissues (Anderson and Sleeman (1995), Keener (1987)) and the effects of cellular heterogeneity in collections of pancreatic β-cells (Sherman et al. (1988), Smolen et al. (1993)) for which gap junction conductances have been measured (Perez et al (1991), Mears et al (1995)). When the coupling is of nearest neighbour type, however, (2)-(3) can be viewed as a center difference approximation of an appropriate reaction diffusion system (Pernarowski (1998)). In such systems, gap junction coupling is replaced with a diffusion term and cell to cell heterogeneity is modelled by imposing a space dependence on parameters which define the single cell model.

In this manuscript we examine just such a class of models:

$$\frac{\partial u}{\partial t} = \nabla \cdot (D(x)\nabla u) + f(u, c, x) - \mu w \quad , \quad D \geq 0 \quad , \tag{4}$$

$$\frac{\partial w}{\partial t} = \nu(g(u, c, x) - w) \quad , \tag{5}$$

$$\frac{\partial c}{\partial t} = \varepsilon h(u, c, x) \quad , \quad 0 < \varepsilon \ll 1 \tag{6}$$

where $\phi = \phi(x,t)$ for $\phi = u, w, c$; $\mu \in \mathbb{R}$, $x \in \Omega \subset \mathbb{R}^3$, Ω is a bounded domain and $t > 0$. Here $u(x,t)$ is a (transformed) membrane potential of a cell at position x, $w(x,t)$ is an activation variable associated with voltage gating of some ionic channel and $c(x,t)$ is the value of a slowly varying regulatory variable. The parameter ν is included to account for a time constant that is often included in (5) in similar models. Moreover, since cells on the boundary $\partial\Omega$ of the spatial domain Ω are not connected to any cells outside Ω by gap junctions,

$$\frac{\partial u}{\partial n} = \nabla u \cdot \hat{N}|_{\partial\Omega} = 0 \quad , \tag{7}$$

where $\hat{N}$ is a unit outward normal to $\partial\Omega$. This boundary condition implies that current cannot flow from intracellular spaces into extracellular regions outside Ω through gap junctions at the boundary.

By defining the functions f, g and h appropriately, the system (4)-(7) can be viewed as a model of electrical activity of a pancreatic islet comprised of many insulin secreting β-cells (Pernarowski (1998)). For example, the Sherman-Rinzel-Keizer model of individual β-cell electrical activity (Sherman et al. (1988)) could be used to define these functions if the relaxation time associated with the voltage rectified potassium current is approximated by a constant.

In this study, we have two objectives. Firstly, by assuming $D = O(\varepsilon^{-1}), 0 < \varepsilon \ll 1$, uniformly on Ω we derive averaged fast and slow subsystems for (4)-(7) with very few assumptions made on the functions f, g and h. Secondly, we apply this general theory to a specific model which mimics the electrical activity of the pancreatic islet. For the latter objective, we use the functions f, g and h defined in Pernarowski (1998) to demonstrate how heterogeneous collections of strongly coupled bursting and beating cells exhibit synchronous behavior in u which is either bursting or beating exclusively. Leading-order thresholds between these synchronous behaviors are derived by an examination of the averaged fast subsystem for the aggregate.

This latter objective addresses an issue discussed in Smolen et al. (1993) where numerical studies demonstrated how β-cells collectively may exhibit synchronous bursting behavior even if some cells when uncoupled would naturally spike but not burst. This contrasting behavior between individual β-cells and β-cell aggregates has been observed experimentally. In Falke et al. (1989), isolated β-cells were observed to beat intermittently (cf. Figure 2a for an example of a periodic beating solution). For other experimental protocols (Smith et al. (1990)), isolated β-cells were observed to burst (cf. Figure 1a for an example of a bursting solution). However, β-cells when intact in the islet were observed to exhibit synchronous bursting behavior (Meda et al. (1984), Meissner (1976)).

In section 2, the dynamics of bursting and beating in a single cell model are described. The parameter regimes for which the model exhibits these behaviors have been determined in other studies (Pernarowski (1994), De Vries (1998)). Key features of those analyses are summarized so that this information can be used to examine the coupled system.

In section 3, averaged fast and slow subsystems are derived for the general system (4)-(7). This theory is then applied in section 4 to a (phenomenological) spherical islet model whose heterogeneities are assumed to be radially symmetric. Lastly, in section 5, a specific heterogeneity is used to compute thresholds between synchronous beating and bursting solutions of the strongly coupled islet. There, cells are assumed to either burst or beat when uncoupled and the leading-order fraction of cells in the aggregate at which synchronous behavior changes from bursting to beating is computed. These asymptotic estimates are then verified numerically using a finite difference method to solve (4)-(7).

2. BURSTING AND BEATING

In this section we describe the single cell (phenomenonological) model to be used later sections. Although the spatial averaging techniques described in section 3 can be applied to Hodgkin-Huxley conductance-based models, we shall instead use the model given by

$$\frac{du}{dt} = f(u) - w - c, \tag{8}$$

$$\frac{dw}{dt} = g(u) - w, \tag{9}$$

$$\frac{dc}{dt} = \varepsilon(h(u) - c) \quad , \quad 0 < \varepsilon \ll 1, \tag{10}$$

to illustrate those procedures on.

In analogy to other β-cell models, the variables u, w and c in (8)-(10) represent, respectively, the transmembrane potential, the activation variable for the voltage-gated potassium current, and a slowly varying regulatory variable (e.g. total free calcium concentration, ATP/ADP ratio). The functions f, g and h are defined in the Appendix. The complicated dependence of the coefficients of these polynomials on the model parameters arises because they are derived (Pernarowski 1998) from a Lienard form for which bifurcation calculations are optimized (see Pernarowski (1994) and De Vries (1998), for instance).

The fast subsystem of (8)-(10) is

$$\frac{du}{dt} = f(u) - w - c, \tag{11}$$

$$\frac{dw}{dt} = g(u) - w, \tag{12}$$

in which c is a bifurcation parameter. It is easily verified that the location of the equilibria of (11)-(12) do not depend on any of the parameters defining f and g (Pernarowski (1994,1998)). The location, number and criticality of Hopf points and the location of homoclinic orbits does, however, depend on the (fast) parameters $(\hat{u}, \eta)$. This dependence has been examined and categorized in great detail (Pernarowski (1994), De Vries (1998)). Throughout this manuscript only η will be varied. Other parameters will have the values $(a, \hat{u}, \beta, u_\beta, \varepsilon) = (1/4, 3/2, 4, -0.954, 0.0025)$.

In Figure 1b, AUTO (Doedel, (1981)) was used to numerically compute the bifurcation diagram in c for $\eta = 0.75$. The Z-shaped locus of equilibria has an upper, middle and lower branch. The lower branch ($u < -1$) and middle branch ($-1 < u < 1$) equilibria are stable nodes and saddles, respectively. Stable periodic solutions are observed to emanate from a supercritical Hopf bifurcation HB on the upper branch ($u > 1$) equilibria. These periodic solutions terminate at a homoclinic bifurcation at $c = c_{HC} > c_m$ where $c_m = 1$ is the value of c at the

saddle-node bifurcation of equilibria at point A. The homoclinic orbit at $c = c_{HC}$ is the result of a transverse intersection of stable and unstable manifolds from the middle equilibria (saddles).

For this same value of η the solution of (8)-(10) was numerically computed. For this simulation, $u(t)$ is depicted in Figure 1a and $(u(t), w(t), c(t))$ is projected onto Figure 1b. It is evident from Figure 1b that the bursting pattern shown in Figure 1a is a consequence of the bistability of the fast subsystem for $c_m < c < c_{HC}$. Above the c nullcline, $\frac{dc}{dt} > 0$ so that $c(t)$ increases along the manifold of limit cycles of the fast subsystem. Likewise, below the c nullcline, $c(t)$ decreases along the stable lower branch of fast subsystem equilibria. In this silent phase, the dynamics of (u, c) in (8)-(10) are found (to leading-order) from the slow subsystem

$$f(u) - g(u) - c = 0, \tag{13}$$

$$\frac{dc}{d\tilde{t}} = h(u) - c, \tag{14}$$

where $\tilde{t} = \varepsilon t$ is a slow time. The existence of periodic bursting solutions of this type has been proven in Terman (1991) provided the fast subsystem and c nullcline are as depicted in Figure 1b.

Analogous diagrams are presented in Figure 2 for $\eta = 0.95$. For this value of η the location of the fast subsystem equilibria is the same but the Hopf point location has changed. Moreover, the periodic solutions emanating from HB terminate at the saddle-node point located at $c = c_m$. Detailed numerical calculations at this point (not shown here) suggest the existence of a degenerate homoclinic orbit which is tangent to the center direction as $t \to -\infty$. The resulting beating solution of (8)-(10) is shown in Figure 2a and appears in a thin vertical strip in the projection in Figure 2b.

Comparing Figure 1b and Figure 2b, the transition from bursting to beating is seen to be a consequence of a loss of bistability in the fast subsystem as η increases. The value η^* of η at which this transition occurs was approximated in Equation (5.44) of Pernarowski (1994) using Melnikov theory as the solution of

$$\eta^2 - (\hat{u} - 3/2)^2 = 3/4. \tag{15}$$

For the value $\hat{u} = 3/2$ used in this manuscript this yields $\eta^* \simeq \eta_{Mel} = \sqrt{3}/2$. As a numerical verification of this approximation, AUTO was used to numerically approximate η^*. To do this, a large period orbit of the fast subsystem (period $T = 30$) was computed for $\eta = 0.75$ (bursting scenario). This periodic solution was used as an approximation of the homoclinic orbit and then continued in the (η, c)-plane (cf. Figure 3). A numerical approximation of the transition value η^* is then found where this continuation curve intersects $c = c_m = 1$. Any numerical approximation so obtained is accurate only in so much as the large period orbit well approximates the homoclinic orbit. In Figure 3, the continuation curve dropping

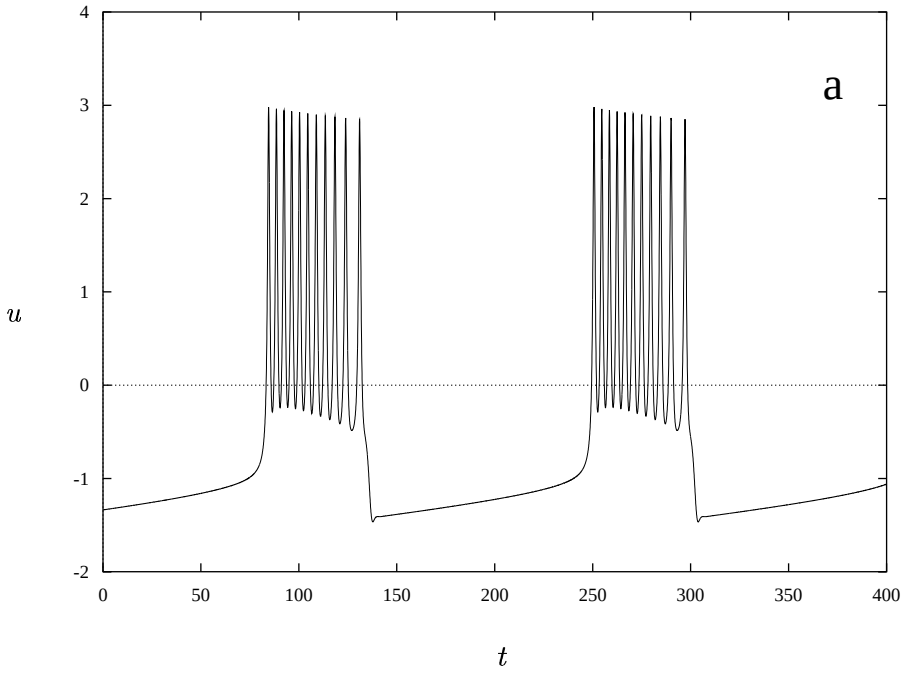

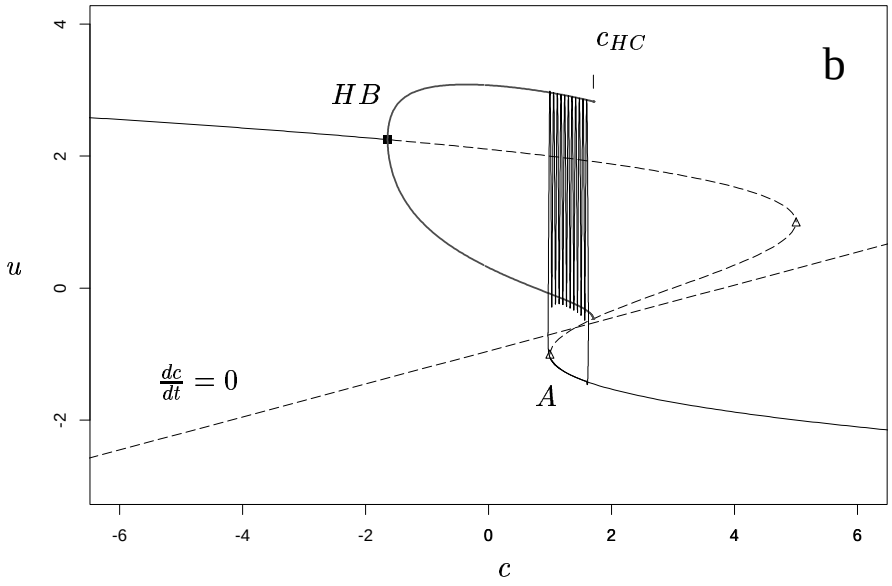

Figure 1. a) shows a square wave bursting solution $u(t)$ for $\eta = 0.75$. b) shows the corresponding fast subsystem diagram. Hopf point (HB) is indicated by a solid square. Open triangles are limit points. Note the stable period solutions (thick solid lines) emanating from HB terminate at a homoclinic bifurcation at $c = c_{HC}$.

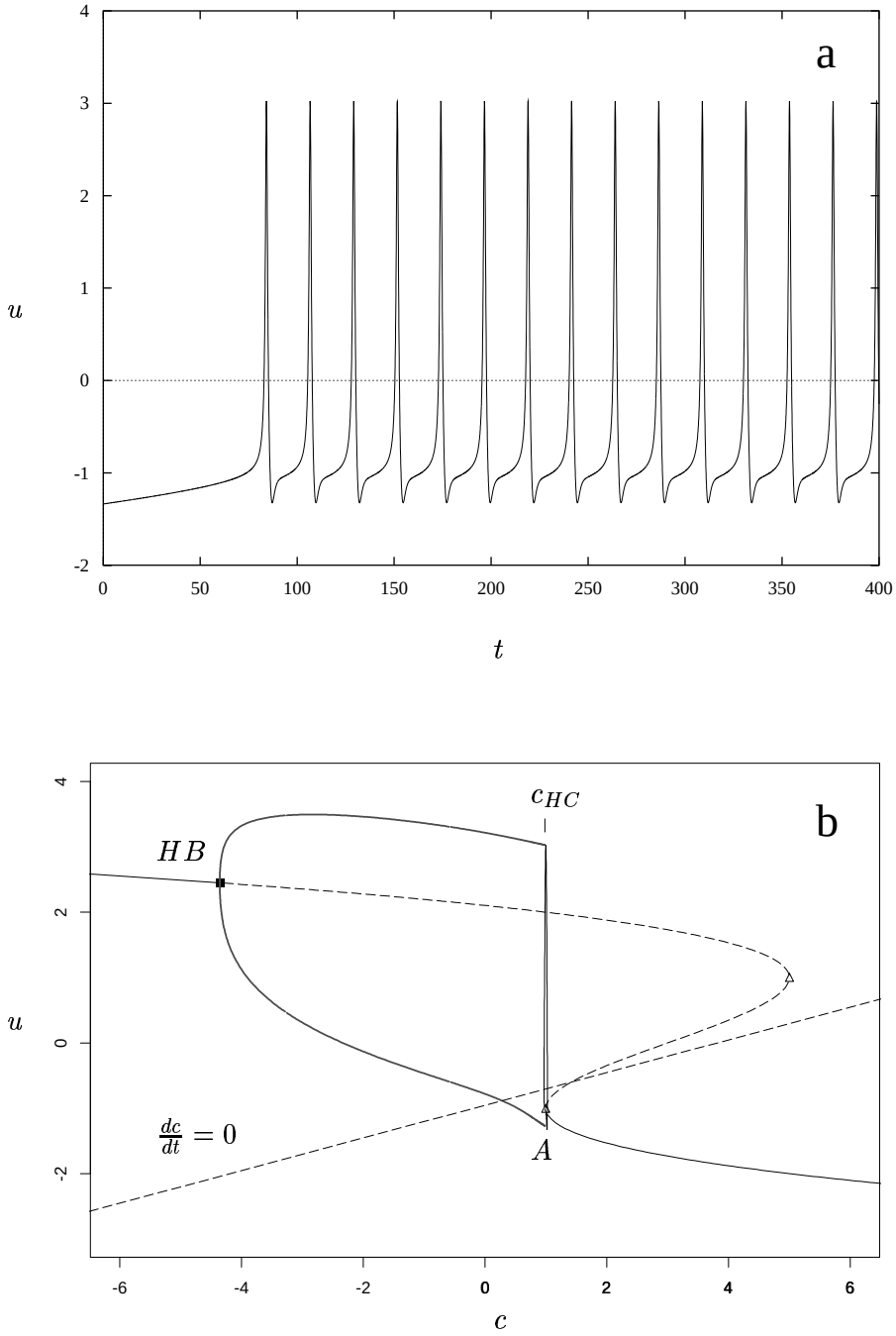

Figure 2. a) shows a beating solution $u(t)$ for $\eta = 0.95$. b) shows the corresponding fast subsystem diagram. Hopf point (HB) is indicated by a solid square. Open triangles are limit points. Note the stable periodic solutions (thick solid lines) emanating from HB terminate at a homoclinic bifurcation at $c = c_m = c_{HC}$.

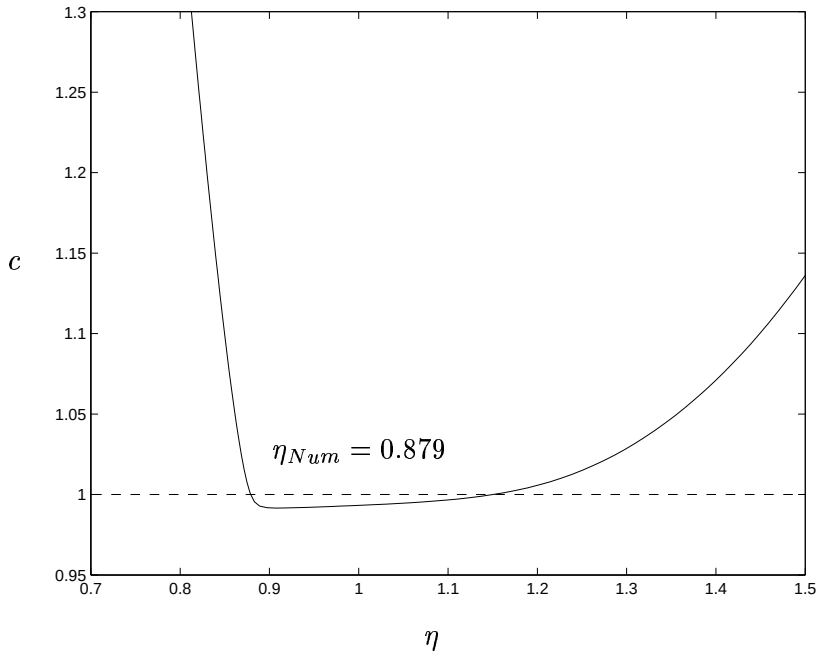

Figure 3. Numerical approximation of threshold between bursting and beating. Solid curve is a two-parameter continuation of an approximate homoclinic orbit. The indicated crossing at $c = c_m = 1$ yields a numerical approximation η_{Num} of the transitional value η^* between bursting and beating solutions.

below $c = c_m = 1$ is an indication of an inaccuracy in this approximation since analytically one expects a continuum of homoclinics along $c = c_m$ for a range of η values above η^* in the beating regime. For the period $T = 30$ used, the transitional value so obtained was $\eta^* \simeq \eta_{Num} = 0.879$ which differs from the asymptotic approximation η_{Mel} by 1.4 %. We use these transition values in section 5 when discussing similar transitions in the heterogeneous spherical islet model.

3. FAST AND SLOW SUBSYSTEMS WITH STRONG COUPLING

In this section we formulate both fast and slow susbsystems of (4)-(7) for the case where $D(x) = O(\varepsilon^{-1})$ and without loss of generality set $D(x) = \varepsilon^{-1}\bar{D}(x)$ with $\bar{D}$ bounded uniformly on Ω. We also assume synchronous initial conditions:

$$u(x,0) = \bar{u} \quad , w(x,0) = \bar{w} \quad , c(x,0) = \bar{c} \quad , \tag{16}$$

where $\bar{u}$,$\bar{w}$ and $\bar{c}$ are constants. The technical issues behind this assumption will be explained at the end of this section.

For the fast subsystem, we assume the regular expansions

$$\phi(x,t) \sim \phi_0(x,t) + \varepsilon\phi_1(x,t) + \ldots \quad , \quad \phi = u, w, c \quad , \tag{17}$$

are valid for times $t = O(1)$. Substitution of (17) into (4)-(6) and (16) yields the leading-order problem

$$\nabla \cdot (\bar{D}(x)\nabla u_0) = 0 \tag{18}$$

$$\frac{\partial w_0}{\partial t} = \nu(g(u_0, c_0, x) - w_0) \tag{19}$$

$$\frac{\partial c_0}{\partial t} = 0 \tag{20}$$

and the $O(\varepsilon)$ problem

$$\frac{\partial u_0}{\partial t} = \nabla \cdot (\bar{D}(x)\nabla u_1) + f(u_0, c_0, x) - \mu w_0, \tag{21}$$

$$\frac{\partial w_1}{\partial t} = \nu(\frac{\partial g}{\partial u}(u_0, c_0, x)u_1 + \frac{\partial g}{\partial c}(u_0, c_0, x)c_1 - w_1) \tag{22}$$

$$\frac{\partial c_1}{\partial t} = h(u_0, c_0, x), \tag{23}$$

where the initial and boundary conditions are:

$$u_0(x,0) = \bar{u} \quad , w_0(x,0) = \bar{w} \quad , c_0(x,0) = \bar{c}, \tag{24}$$

$$u_1(x,0) = 0 \quad , w_1(x,0) = 0 \quad , c_1(x,0) = 0 \quad , \tag{25}$$

$$\nabla u_i \cdot \hat{N}|_{\partial\Omega} = 0, \quad i = 0, 1. \tag{26}$$

We introduce the average notation(s):

$$< \phi(x,t) >= \hat{\phi}(t) = \frac{1}{|\Omega|}\int_\Omega \phi(x,t)dx \quad , \tag{27}$$

where $|\Omega|$ is the volume of Ω and $\phi(x,t)$ is any integrable function.

Clearly, (18) and (26) imply $u_0 = u_0(t)$ where $u_0(0) = \bar{u}$. Moreover, $c_0 = \bar{c}$. Despite these dependences on (x,t) the heterogeneity in (19) implies that w_0 depends both on x and t. By averaging (21) in x, applying the divergence theorem and using the boundary conditions on u_1 we find

$$\begin{aligned} < \tfrac{\partial u_0}{\partial t} >= \tfrac{\partial u_0}{\partial t} \quad &= \tfrac{1}{|\Omega|}\textstyle\int_\Omega \nabla \cdot (\bar{D}(x)\nabla u_1)dx + < f(u_0, c_0, x) > -\mu\hat{w}_0 \\ &= \tfrac{1}{|\Omega|}\textstyle\int_{\partial\Omega} \bar{D}(x)\nabla u_1 \cdot \hat{N}dS + < f(u_0, c_0, x) > -\mu\hat{w}_0 \\ &= < f(u_0, c_0, x) > -\mu\hat{w}_0 \end{aligned}$$

where $\hat{N}$ is a unit vector outwardly normal to the boundary $\partial\Omega$. This result and the average of (19) yields a spatially independent (averaged) fast subsystem:

$$\frac{\partial u_0}{\partial t} = < f(u_0, c_0, x) > -\mu\hat{w}_0 \quad , \tag{28}$$

$$\frac{\partial \hat{w}_0}{\partial t} = \nu(< g(u_0, c_0, x) > -\hat{w}_0) \quad , \tag{29}$$

where $(u_0(0), \hat{w}_0(0)) = (\bar{u}, \bar{w})$. Once the solution $u_0(t)$ has been found, (19) can be integrated to determine $w_0(x,t)$:

$$w_0(x,t) = e^{-\nu t}\left(\bar{w} + \nu\int_0^t e^{\nu s} g(u_0(s), \bar{c}, x)ds\right) \quad . \tag{30}$$

Providing $\frac{\partial g}{\partial x} \neq 0$, it is evident from the explicit dependence of $w_0(x,t)$ on x that $w_0(x,t)$ is nonsynchronous for all $t > 0$. Moreover, one cannot expect that $w_0(x,t)$ is asymptotic to an x-independent (synchronous) solution as $t \to \infty$. To illustrate this, consider the case $g(u,c,x) = G(x)$ where G is any nonzero function whose spatial average is zero, i.e., $< g >=< G(x) >= 0$. Then, from (30) it is easily verified that $w_0(x,t) \sim G(x)$ as $t \to \infty$ for all $\nu > 0$.

For the slow subsystem analysis, we introduce the slow time $\tilde{t} = \varepsilon t$ and assume the expansions

$$\phi(x,t) \sim \Phi_0(x,\tilde{t}) + \varepsilon\Phi_1(x,\tilde{t}) + \ldots \quad , \quad \phi = u, w, c \quad , \tag{31}$$

are valid for times $\tilde{t} = O(1)$. Substitution of (31) into (4)-(6)

$$\nabla \cdot (\bar{D}(x)\nabla U_0) = 0, \tag{32}$$

$$W_0 = g(U_0, C_0, x), \tag{33}$$

$$\frac{\partial C_0}{\partial \tilde{t}} = h(U_0, C_0, x), \tag{34}$$

and the $O(\varepsilon)$ problem

$$\nabla \cdot (\bar{D}(x)\nabla U_1) = \mu W_0 - f(U_0, C_0, x), \tag{35}$$

$$\frac{\partial W_0}{\partial \tilde{t}} = \nu(\frac{\partial g}{\partial u}(U_0, C_0, x)U_1 + \frac{\partial g}{\partial c}(U_0, C_0, x)C_1 - W_1), \tag{36}$$

$$\frac{\partial C_1}{\partial \tilde{t}} = \frac{\partial h}{\partial u}(U_0, C_0, x)U_1 + \frac{\partial h}{\partial c}(U_0, C_0, x)C_1, \tag{37}$$

Initial and boundary conditions are as in (24)-(26) with lower case characters replaced by uppercase characters.

Once again, $U_0 = U_0(\tilde{t})$, i.e., U_0 only depends on $\tilde{t}$ and not x. Furthermore, simultaneously averaging (33) and (35) and then applying the divergence theorem with boundary conditions for U_1, $\hat{W}_0$ can be eliminated to obtain the requirement that

$$F \equiv < f(U_0, C_0, x) - \mu g(U_0, C_0, x) >= 0. \tag{38}$$

The averaged slow subsystem for the model would then be (38) and the average of (34):

$$\frac{\partial \hat{C}_0}{\partial \tilde{t}} =< h(U_0, C_0, x) > \tag{39}$$

Even though U_0 depends only on $\tilde{t}$, C_0 may depend on x. However, if $h_x = 0$ then $< h(U_0, C_0, x) >$ is solely a function of (U_0, C_0) so that C_0 depends only on $\tilde{t}$. In this case, F in (38) is also a function of (U_0, C_0) and (38),(39) form a spatially independent slow subsystem. A case where $h_x \neq 0$ was considered in Pernarowski (1998). In the next section we consider a specific model for which both fast and slow averaged subsystems are spatially independent.

Lastly, we explain the technical issues behind the assumed synchronous initial conditions (16). Suppose we assumed $u(x, 0) = \bar{u}(x)$ is not constant and that the expansion (17) is valid for times $t = O(1)$. Then $u_0(x, t)$ must satisfy

$$\nabla \cdot (\bar{D}(x) \nabla u_0) = 0, \quad x \in \Omega, t > 0, \tag{40}$$

$$\nabla u_0 \cdot \hat{N}|_{\partial\Omega} = 0, \tag{41}$$

$$u_0(x, 0) = \bar{u}(x), \quad x \in \Omega. \tag{42}$$

Solutions of (40)-(41) differ at most by a function of t (Kevorkian (1992)). Thus, solutions of (40)-(41) must be solely a function of t, i.e., $u_0(x, t) = u_0(t)$. Therefore, unless $\bar{u}(x)$ is constant, the last equation (42) cannot be satisfied for all $x \in \Omega$ at $t = 0$. In short, if the initial condition for u is assumed not to be constant then the assumed expansion (17) results in a leading problem for u_0 which has no solution. This implies that (17) is an inappropriate expansion for capturing any rapid synchronization of $u(x, t)$ from an initially nonsynchronous state. An appropriate asymptotic expansion for nonsynchronous initial conditions would have two times:

$$\phi(x, t) \sim \phi_0(x, t, \hat{t}) + \varepsilon \phi_1(x, t, \hat{t}) + \ldots \quad , \quad \phi = u, w, c \quad , \tag{43}$$

where the initial synchronization of u would occur on the very fast time scale $\hat{t} = t/\varepsilon$. Rather than explore the tractibility of a two-time analysis for nonsynchronous initial conditions, the assumptions (16)-(17) were used to derive averaged fast and slow subsystems sufficient for predicting the type of synchronous behavior which results from an imposed heterogeneity. This is the topic of section 5.

4. SPHERICAL ISLET MODEL

In this section, we derive fast and slow subsystems for a model of electrical activity in a spherical pancreatic islet of radius R. For simplicity, we will examine the case where heterogeneities are radially symmetric and that the resulting solution is also radially symmetric. The specific model we examine is:

$$\frac{\partial u}{\partial t} = \frac{1}{\varepsilon r^2}\frac{\partial}{\partial r}\left(D(r)r^2\frac{\partial u}{\partial r}\right) + f(u;\lambda(r)) - w - c \quad , 0 < r < R, \tag{44}$$

$$\frac{\partial w}{\partial t} = g(u;\lambda(r)) - w, \tag{45}$$

$$\frac{\partial c}{\partial t} = \varepsilon(h(u;\lambda(r)) - c), \tag{46}$$

where f,g and h are defined in the Appendix, $\phi = \phi(r,t), \phi = u, w, c$, and the parameters $\lambda = (\hat{u}, \eta, a, \beta, u_\beta)$ have some known dependence on r. Since the solution is bounded and radially symmetric on a spherical domain, the boundary conditions are:

$$\frac{\partial u}{\partial r}(x,t) = 0 \quad , x = 0^+, R. \tag{47}$$

Using the theory developed in the preceding section it is easily seen that the space-independent fast subsystem corresponding to (44)-(46) is:

$$\frac{\partial u_0}{\partial t} = < f(u_0;\lambda(r) > -\hat{w}_0 - c_0 \quad , \tag{48}$$

$$\frac{\partial \hat{w}_0}{\partial t} = < g(u_0;\lambda(r)) > -\hat{w}_0 \quad , \tag{49}$$

and $c_0 = \bar{c}$ is constant. Since u_0 only depends on t, the spatial averages in (48)-(49) only affect the coefficients of f and g. Hence, both $< f(u_0;\lambda(r)) >$ and $< g(u_0;\lambda(r) >$ are constant coefficient cubics in u_0. Defining

$$\hat{f}(u) = \sum_{i=1}^{3} < f_i(r) > u^i, \tag{50}$$

$$\hat{g}(u) = \sum_{i=0}^{3} < \omega_i(r) > u^i, \tag{51}$$

(48)-(49) may be written as the autonomous system of ordinary differential equations

$$\frac{du_0}{dt} = \hat{f}(u_0) - \hat{w}_0 - c_0 \quad , \tag{52}$$

$$\frac{d\hat{w}_0}{dt} = \hat{g}(u_0) - \hat{w}_0 \quad , \tag{53}$$

whose dynamics will be known once $< f_i(r) >$ and $< \omega_i(r) >$ have been computed.

For the slow subsystem we note given $\mu = 1$ and the definitions of f and g in the Appendix, (38) becomes

$$F = -U_0^3 + 3(U_0 + 1) - \hat{C}_0 = 0. \tag{54}$$

Similarly, given U_0 depends only on $\tilde{t}$, averaging (34) in r one finds

$$\frac{d\hat{C}_0}{d\tilde{t}} = \hat{\beta}U_0 - < \beta u_\beta > -\hat{C}_0 \tag{55}$$

For given heterogeneities in β and u_β the slow subsystem (54)-(55) is a differential-algebraic problem which can be solved explicitly. This was done in Pernarowski (1998) where the effect that heterogeneities in the slow subsystem parameters (β, u_β) had on global behavior was examined. There, the leading-order synchronous behavior of the membrane potential $u(x,t)$ was shown to either exhibit bursting or steady state behavior depending on the fraction of cells having parameter values $\beta(x)$ in the steady state regime. Global behavior can also be altered by heterogeneities in "fast parameters" (parameters which occur solely in the fast subsystem but not the slow subsystem). This we demonstrate in the next section.

5. BEATERS VERSUS BURSTERS

In this section we illustrate, by way of example, how fast subsystem heterogeneities can affect global behavior in (44)-(46). For the spherical islet model we fix all parameters [†] except for η for which we impose the heterogeneity

$$\eta(r) = \begin{cases} \eta_a & 0 < r < \rho R \\ \eta_b & \rho R < r < R \end{cases}, \tag{56}$$

where $\rho \in [0,1]$. The constants $\eta_a = 0.75$ and $\eta_b = 0.95$ were chosen so that the corresponding single cell model ($D = 0$) with $\lambda = \lambda_a = (\hat{u}, \eta_a, a, \beta, u_\beta)$ and $\lambda = \lambda_b = (\hat{u}, \eta_b, a, \beta, u_\beta)$ exhibit bursting and beating behaviors, respectively. With these definitions, (44)-(46) and (56) model a pancreatic islet consisting of bursting cells on the interior of the islet ($0 < r < \rho R$) with the remainder cells beaters. The question we address is: given strong coupling, at what critical value of $\rho = \rho^*$ does the synchronous behavior of u change from beating to bursting?

The fact that u is synchronous (to leading-order) follows from u_0 and U_0 depending only on t and $\tilde{t}$, respectively. Examining the definitions of f and g in the

[†] at the aformentioned values $(a, \hat{u}, \beta, u_\beta, \varepsilon) = (1/4, 3/2, 4, -0.954, 0.0025)$.

Appendix, the heterogeneity (56) is seen to affect only the coefficients f_1 and ω_1 in (50)-(53). Moreover, defining the quantity

$$\tilde{\eta} =< \eta(r)^2 >^{1/2} \tag{57}$$

we note that the fast subsystem (52)-(53) (and slow subsystem) has a bifurcation structure in the $(\tilde{\eta}, \hat{u})$-plane identical to the fast subsystem (11)-(12) of the single cell model in the $(\eta, \hat{u})$-plane. Thus, the value ρ^* of ρ at which a transition between synchronous beating and bursting occurs can be obtained by solving $\tilde{\eta} = \eta^*$ (see section 2 for a definition of η^*).

For a spherical islet of radius R we note that the average of any function $\phi(r)$ is given as

$$\hat{\phi} = \frac{3}{R^3} \int_0^R r^2 \phi(r) dr. \tag{58}$$

Given (56), $\tilde{\eta}$ is easily computed

$$\tilde{\eta} = \tilde{\eta}(\rho) = \sqrt{\eta_b^2 - (\eta_b^2 - \eta_a^2)\rho^3}. \tag{59}$$

Solving $\tilde{\eta}(\rho) = \eta^*$ we obtain

$$\rho^* = \left(\frac{\eta_b^2 - \eta^{*2}}{\eta_b^2 - \eta_a^2} \right)^{1/3}. \tag{60}$$

To convert this to a volume equivalent, we note that the proportion of the total islet volume occupied by bursters is ρ^3. Thus, the transitional volume fraction is

$$V^* = (\rho^*)^3 = \frac{\eta_b^2 - \eta^{*2}}{\eta_b^2 - \eta_a^2} \tag{61}$$

Depending on the values of (η_a, η_b), V^* can attain any value in the interval $(0, 1)$. As $\eta_a \to \eta^{*-}$, $V^* \to 1^-$. Similarly, as $\eta_b \to \eta^{*+}$, $V^* \to 0^+$.

Using the values η_{Mel} and η_{Num} obtained in section 2 to (asymptotically) approximate η^* we obtain from (61) the transition values $V^*_{Mel} = 0.45$ and $V^*_{Num} = 0.39$, respectively. Since

$$\left(\frac{\rho + \Delta\rho}{\rho} \right)^3 \geq \frac{\rho + \Delta\rho}{\rho} \quad , \quad 1 \geq \rho + \Delta\rho \geq \rho > 0,$$

the relative error in the corresponding ρ values is expectedly smaller ($\rho^*_{Mel} = 0.765$ and $\rho^*_{Num} = 0.730$, respectively).

To verify these asymptotic results numerically, a finite difference scheme was used to compute solutions of the model equations. Standard centered difference approximations of derivatives were used at all grid points except at the origin. To

handle the singularity in the Laplacian at the origin, the development in Morton and Mayers (1994) was applied. Letting $u_i(t) = u(r_i, t), r_i = i\Delta r, \Delta r = R/n, i = 0, \ldots n$, this procedure yields the following discretization of (44)

$$\dot{u_0} = f_0 - w_0 - c_0 + 6\gamma(u_1 - u_0) \tag{62}$$

$$\dot{u_i} = f_i - w_i - c_i + \gamma(u_{i-1} - 2u_i + u_{i+1}) + \frac{\gamma}{i}(u_{i+1} - u_{i-1}) \quad i \neq 0, n \tag{63}$$

$$\dot{u_n} = f_n - w_n - c_n + 2\gamma(u_{n-1} - u_n) \tag{64}$$

where $\gamma = \frac{D}{\varepsilon \Delta r^2}$ and $f_i = f(u_i, \lambda(r_i))$. This system of ordinary differential equations (and the corresponding equations for w and c) were then integrated in time using a stiff equation solver.

In Figure 4 we present grey scale contours of the numerical approximations for $u(r, t)$ at different ρ values. As anticipated from the asymptotic results, these figures illustrate synchronous beating (cf. Figure 4a) and bursting behaviors (cf. Figure 4b) despite the imposed heterogeneities on η. In direct simulations, the transition point ρ^* was defined as the ρ value at which the synchronous behavior in u changes from a two spike burster to a single spike beater. Two spike bursters were distinguished from two periods of a beater by noting the local minima of the active phase spikes in bursters are above the saddle node point A of Figure 1b and thus have $u > -1$. Through repetitive integrations with different ρ values a binary search using these criteria resulted in $\rho^* \simeq 0.79$. This value does not differ too greatly from ρ^*_{Mel} and ρ^*_{Num} which, being asymptotic estimates, have an expected increase in accuracy only as $\varepsilon \to 0$.

6. DISCUSSION

The differing electrical activity of isolated pancreatic β-cells and β-cells in intact islets led Smolen et al (1993) to conjecture that these differences may be a consequence of cell-cell heterogeneity. The asymptotic techniques applied herein support numerical results in that study when the coupling is strong. These techniques were illustrated on a heterogeneous collection of beaters and bursters to further emphasize the plausibility of the heterogeneity conjecture. The dependence of islet electrical activity on coupling strength which was also studied numerically in Smolen et al (1993) cannot be explained using the analysis herein since the asymptotic methods are valid only if $D \gg 1$.

It should be stressed that the asymptotic techniques described here can be applied to any strongly coupled collections of (any type of) cells whose electrical activity can be modelled by (4)-(6). In this more general setting we note that the results show a) electrical activity u is synchronous despite cell-cell heterogeneity and b) the behavior of the resulting synchronous electrical activity can be understood via appropriately averaged fast and slow subsystems. On the latter issue some careful distinctions must be made. First and foremost, the appropriate averaged fast

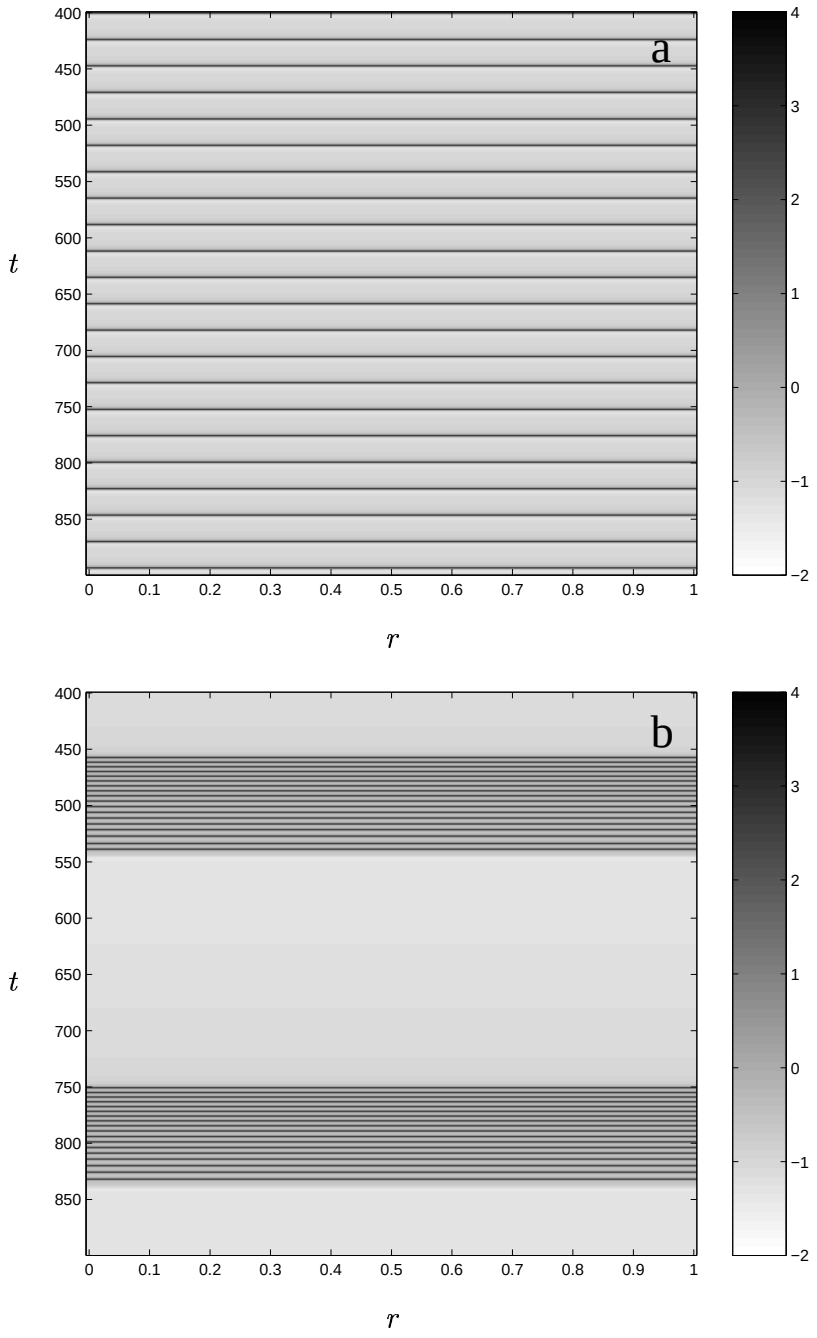

Figure 4. Numerical solutions of $u(r,t)$ in spherical islet model for $(D,n,R) = (10,100,1)$: a) has $\rho = 0.05$ shows a synchronous beating pattern whereas b) has $\rho = 0.95$ and shows a synchronous bursting pattern. In both cases, the pattern is synchronized in r despite heterogeneities in $\eta(r)$ since gap junction coupling is strong.

and slow subsystems are not (in general) obtained by simply replacing the parameters by their spatial averages. For example, the averaged fast subsystem in section 5 was the same as the single cell model fast subsystem if $\eta(x)$ was replaced by $< \eta(x)^2 >^{1/2}$ and not $< \eta(x) >$. Secondly, depending on the underlying single cell model and the type of heterogeneity, the averaged fast and slow subsystems may not even be ordinary differential equations. For the class of models examined in section 4, the averaged fast and slow subsystems had exactly the same form as the single cell model if h_r=0. This made it possible to predict transitional values between synchronous beating and bursting behaviors in section 5. For other models, however, there may not be functions $\hat{f} = \hat{f}(u)$ and $\hat{g} = \hat{g}(u)$ such that $\hat{f} =< f(u,x) >$ and $\hat{g} =< g(u,x) >$. For such models, the averaged fast subsystem cannot be obtained by replacing model parameters with appropriate averages. Despite these issues, many heterogeneous maximal conductances $\bar{g}_X$ associated with the currents I_X in (2) can be replaced by their spatial averages. This would be true for all currents I_X with the functional form $I_X = \bar{g}_X i_x(v)$ (such as quasi-steady state voltage gated currents and leakage currents) providing the remaining parameters defining i_x were spatially homogeneous.

Hale and Sakamoto (1989) have examined the approach to synchronous solutions in the context of homogenous (x-independent) reaction diffusion models when diffusivity is large. Applicability of their results to specific models depends on knowing the existence and stabilty characteristics of global attractors in the corresponding "shadow" system. In that study, the original system is proven to have the same attractors as the shadow, or spatially averaged, system. The analysis is based on a careful examination and comparison of the flows of each system in appropriate Banach spaces. In contrast, here we have outlined an asymptotic procedure for deriving averaged fast and slow subsystems in a heterogeneous (x-dependent) reaction diffusion model whose diffusivity is large. These asymptotic procedures do not constitute a proof that the solutions of (4)-(6) synchronize to periodic solutions (bursters, beaters) described by the averaged fast and slow subsystems. The results herein, however, suggest that the methods used by Hale and Sakamoto (1989) might be adapted with appropriate modifications.

Such synchrony results would greatly depend on the fact that coupling is strong. Indeed, if coupling is weak, solutions need not synchronize. This is demonstrated numerically in Sherman and Rinzel (1992) where a model of two weakly coupled cells is shown to possess stable antiphase (periodic) solutions. In a study by Manor et al (1997) a different coupled two cell model is examined using both asymptotic and numerical approaches. There, the Lindstedt-Poincare method (see Kevorkian (1990)) is used to examine synchrony in the fast subsystem when coupling is strong.

Future studies with regard to fast-slow subsystem descriptions for models of the type (4)-(6) can be divided roughly into three categories: $D = O(1/\varepsilon)$, $D = O(1)$, and $D = O(\varepsilon)$. This study and the companion paper (Pernarowski (1998)) represent initial studies for the first case. For the last case, interesting solutions

may occur primarily because smallness of diffusivity can lead to boundary-layer phenomena. If $D = O(\varepsilon)$ however, the continuum approximation

$$Du_{xx} \simeq \gamma(u_{i+1} - 2u_i + u_{i-1})$$

for gap junction coupling may no longer hold. This is evident by the fact that numerical schemes based on the above center difference approximation of second derivatives converge only if the grid spacing $\Delta x \to 0$ (or equivalently $\gamma = D/\Delta x^2 \to \infty$).

For the case $D = O(1)$, fast-slow subsystem analyses of (4)-(6) is significantly more complicated. To illustrate this, note that if $D = O(1)$ and there is no heterogeneity, the fast subsystem of (4)-(6) in a one dimensional spatial domain is

$$u_t = Du_{xx} + f(u, c) - \mu w \ , \tag{65}$$

$$w_t = g(u, c) - w \tag{66}$$

The steady state structure of this reaction-diffusion system can depend on the value of D. Turing bifurcations for instance could give rise to additional equilibria. It is therefore possible that bistability in the bifurcation parameter c could be lost. Examinations of these and other issues will be left for later studies.

7. ACKNOWLEDMENT

The author wishes to thank W. Pursell for computing the finite difference approximations for the spherical islet model in section 5.

8. APPENDIX

$$f(u) = f_3 u^3 + f_2 u^2 + f_1 u + f_0 \quad , \tag{67}$$

$$f_3 = -\frac{a}{3} \quad , \tag{68}$$

$$f_2 = a\hat{u} \quad , \tag{69}$$

$$f_1 = 1 - a(\hat{u}^2 - \eta^2) \quad , \tag{70}$$

$$f_0 = 0, \tag{71}$$

$$g(u) = \omega_3 u^3 + \omega_2 u^2 + \omega_1 u + \omega_0 \quad , \tag{72}$$

$$\omega_3 = f_3 + 1 = 1 - \frac{a}{3} \quad , \tag{73}$$

$$\omega_2 = f_2 \quad , \tag{74}$$

$$\omega_1 = f_1 - 3 = -a(\hat{u}^2 - \eta^2) - 2 \quad , \tag{75}$$

$$\omega_0 = -3 \quad . \tag{76}$$

and

$$h(u) = \beta(u - u_\beta) \tag{77}$$

9. REFERENCES

Anderson, A.R., B.D. Sleeman. 1995. Wavefront propagation and its failure in coupled systems of discrete bistable cells modelled by FitzHugh-Nagumo dynamics. *Int. J. Bif. Chaos* 5:63-74.

Bertram, R., P. Smolen, A. Sherman, D. Mears, I. Atwater, F. Martin. 1995. A role for calcium release-activated current (CRAC) in cholinergic modulation of electrical activity in pancreatic β-cells. *Biophys. J.* 68:2323-2332.

De Vries, G., R.M. Miura. 1998. Analysis of a class of models of bursting electrical activity in pancreatic β-cells. *SIAM J. Appl. Math.* 58:607-635.

De Vries, G. 1998. Multiple Bifurcations in a polynomial model of bursting oscillations. *J. Nonlinear Sc.* 8:281-316.

Doedel, E. J., AUTO: A program for the automatic bifurcation and analysis of autonomous systems, in *Proc. 10th Manitoba Conf. on Numer. Math. and Comput.*, Winnepeg, Canada, Congr. Numer., 30 (1981) pp. 265-284.

Falke, L.C., K.D. Gillis, D.M. Pressel, S. Misler. 1989. Perforated patch recording allows long-term monitoring of metabolite-induced electrical activity and voltage-dependent Ca^{2+} currents in pancreatic B cells. *FEBS (Fed. Eur. Biochem. Soc.) Lett.* 251:167-172.

Hale, J.K., K. Sakamoto. 1989. Shadow systems and attractors in reaction-diffusion equations. *Applicable Analysis* 32:287-303.

Hille, B. 1992. Ionic Channels of Excitable Membranes. *Sinauer Associates Inc., Sunderland, Massachuesetts.*

Keener, J. P. 1987 Propagation and its failure in coupled systems of discrete excitable cells. *SIAM J. Appl. Math.* 47:556-572.

Kevorkian, J. 1990. Partial Differential Equations: Analytical Solution Techniques. Wadsworth & Brooks/Cole Advanced Books, Pacific Grove, California.

Manor, Y., J. Rinzel, I. Segev, Y. Yardom. 1997. Low-amplitude oscillations in the inferior olive: a model based on electrical coupling of neurons with heterogeneous channel densities. *J. Neurophysiol.* 77:2736-2752.

Mears, D., N.F. Sheppard, Jr., I. Atwater, E. Rojas. 1995. Magnitude and modulation of pancreatic β-cell gap junction electrical conductance in situ. *J. Membrane Biol.* 146:163-176.

Meda, P., I. Atwater, A. Goncalves, A. Bangham, L. Orci, E. Rojas. 1984. The topography of electrical synchrony among B-cells in the mouse islets of Langerhans. *Q. J. Exp. Physiol.* 69:719-735.

Meissner, H.P. 1976. Electrophysiological evidence for coupling between β-cells of pancreatic islets. *Nature (Lond.)* 262:502-504.

Morton, K.W., D.F. Mayers. 1994. Numerical Solution of Partial Differential Equations, Cambridge University Press.

Perez-Armendariz,M., C. Roy, D.C. Spray, M.V.L. Bennett. 1991. Biophysical properties of gap junctions between freshly dispersed pairs of mouse pancreatic beta cells. *Biophys. J.* 59:76-92.

Pernarowski, M. 1994. Fast subsystem bifurcations in a slowly varying Lienard system exhibiting bursting. *SIAM J. Appl. Math.* 54:814-832.

Pernarowski, M. 1998. Fast and Slow subsystems for a continuum model of bursting activity in the pancreatic islet. *SIAM J. Appl. Math.* 58:1667-1687.

Sherman, A. 1994. Anti-phase, asymmetric and aperiodic oscillations in excitable cells - I. Coupled bursters. *Bull. Math. Biol.* 56:811-836.

Sherman, A., J. Rinzel. 1992. Rhythmogenic effects of weak electrotonic coupling in neuronal models. *Proc. Natl. Acad. Sci.* 89:2471-2474.

Sherman, A., J. Rinzel, J. Keizer. 1988. Emergence of organized bursting in clusters of pancreatic β-cells by channel sharing. *Biophys. J.* 54:411-425.

Smith, P.A., F.M. Aschroft, P. Rorsman. 1990. Simultaneous recordings of glucose dependent electrical activity and ATP-regulated K^+-currents in isolated mouse pancreatic β-cells. *FEBS (Fed. Eur. Biochem. Soc.) Lett.* 261:187-190.

Smolen, P., J. Rinzel, A. Sherman. 1993. Why pancreatic islets burst but single β-cells do not: The heterogeneity hypothesis. *Biophys. J.* 64:1668-1680.